J. Electrochem. Sci. Eng. **12(1)** (2022) 91-103; http://dx.doi.org/10.5599/jese.1117

Open Access : : ISSN 1847-9286

https://pub.iapchem.org/ojs/index.php/JESE

Original scientific paper

Construction of a simple and selective electrochemical sensor based on Nafion/TiO_2 for the voltammetric determination of olopatadine

Mohammad Mehmandoust[1,2,✉], Amirhossein Mehmandoust[3] and Nevin Erk[1,2,✉]

[1]*Department of Analytical Chemistry, Faculty of Pharmacy, Ankara University, Ankara, Turkey*
[2]*Sakarya University, Biomaterials, Energy, Photocatalysis, Enzyme Technology, Nano & Advanced Materials, Additive Manufacturing, Environmental Applications, and Sustainability Research & Development Group (BIOENAMS R&D Group), 54187 Sakarya, Turkey*
[3]*Department of Chemistry, Faculty of Science, Urmia University, 1177, Urmia, Iran*

Corresponding authors: ✉*mehmandoust@ankara.edu.tr and* ✉*erk@pharmacy.ankara.edu.tr*

Received: October 21, 2021; Accepted: October 14, 2021; Published: November 20, 2021

Abstract

A selective and facile voltammetric method based on titanium dioxide nanoparticles and Nafion (Nafion/TiO_2 NPs) on the screen-printed electrode (SPE) was proposed for olopatadine determination. Followed by the synthesis of TiO_2 nanoparticles, various methods, including high-resolution transmission electron microscopy (HR-TEM), ultraviolet-visible spectroscopy (UV-Vis), energy-dispersive X-ray (EDX) Raman spectrum, and electrochemical impedance spectroscopy (EIS) were utilized to characterize the nanomaterials. Nafion/TiO_2 on the screen-printed electrode (NFN/TiO_2/SPE) was used to determine olopatadine in concentration ranges of 0.01 to 0.07 and 0.07 to 14.6 µM with a limit of quantification as low as 7.0 nM, via differential pulse voltammetry technique. The NFN/TiO_2/SPE offered a high-performance ability to determine olopatadine in the eye drop sample with satisfactory recovery data of 98.2–99.0 %. Also, the developed electrode showed good reproducibility, repeatability, and high selectivity features. The obtained results indicate that NFN/TiO_2/SPE could be utilized as an appropriate candidate for electrochemical olopatadine sensing.

Keywords

Monitoring; screen-printed electrode, differential pulse voltammetry.

Introduction

Olopatadine (OLP) is a tricyclic drug that impedes mast cell mediator liberating and possesses histamine H1-receptor antagonist activity. Olopatadine hydrochloride is utilized to treat allergic

conjunctivitis. In vivo and in vitro, a relatively specific histamine H1 antagonist reduces type 1 immediate hypersensitivity, including histamine-induced effects on human conjunctival epithelial cells [1]. The physiologic effect of olopatadine is utilizing decreased histamine release. The IUPAC name of olopatadine is 2-[(11Z)-11-[3-(dimethylamino) propylidene]-6H-benzo[c][1]benzoxepin-2-yl]acetic acid and it is shown in Scheme. 1.

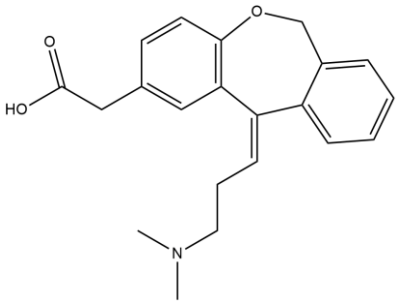

Scheme. 1. *The chemical structure of olopatadine*

Currently, different analytical methods have been proposed to determine olopatadine, including UV–Vis spectrophotometry [2-4] and high-performance liquid chromatography (HPLC) [5, 6]. However, it is worth noting that the current electrode systems, such as screen-printed electrodes (SPE), present significant advantages such as simple operation and portability, compared to the widespread electrode systems such as glassy carbon electrodes [7]. Therefore, it is desirable to fabricate a portable electrochemical sensor to determine antihistamine agents in real samples. In this regard, fabricating an electrode with a novel nanomaterial is essential for electrochemical applications engineering a multi-functional sensing material[8-16].

Nanomaterials showed many advantages in different branches of science [17-24]. In recent years, nanostructured materials, including metal oxides nanoparticles, have been used to fabricate the modified electrodes for biological, pharmaceutical, energy and environmental purposes [25-33]. Among the various nanomaterials, titanium dioxide (TiO_2) has outstanding properties such as appropriate sensitivity and stability for its strong affinity to a phosphate group, photocatalytic effect, porosity, steadiness, and high specific surface areas [34,35]. TiO_2 nanoparticles have also been applied in wide potential windows, improving the electrode's stability, increasing the electrode response's repeatability [36,37]. Combining metallic characteristics' electronic conductivity and electroactivity with Nafion's (NFN) high ionic conductivity and ion-exchange capacity opens up many possibilities for nanoparticle design in NFN modified electrodes with unique features and uses [38]. This study employed the SPE electrodes and the promising development of a susceptible electrochemical sensor based on titanium dioxide nanoparticles and Nafion. It would be expected that the combination of TiO_2 with Nafion could provide excellent electrochemical sensing performance for olopatadine. Titanium dioxide nanoparticles were used to prepare additional improvements because their stated physicochemical features include strong biocompatibility, solid adsorptive ability, large surface area, thermal stability, non-toxicity, and electrical/electrochemical capabilities.

The synergic effect of Nafion and TiO_2 remarkably enhanced the electrocatalytic activity towards the OLP and consequently allowed us to reach its detection limit up to 7.0 nM. Moreover, NFN/TiO_2/SPE exhibited a promising analytical performance in the wide linear concentration ranges of 0.01 to 0.07 and 0.07 to 14.66 µM towards the OLP under optimized experimental conditions. The developed electrochemical sensing platform was successfully utilized to determine the amount of OLP in real samples with satisfactory recovery.

Experimental

Chemical and reagents

All materials were of analytical purity and have not been subjected to a further purification process. C_3H_6O (acetone), C_2H_5OH (ethanol), NaOH (sodium hydroxide) were supplied from Merck (Darmstadt, Germany). L-ascorbic acid (99.0 %), L-cysteine (97.0 %), L-arginine (98.0 %), dopamine hydrochloride (99.0 %), glucose (99.5 %), uric acid (99.0 %), potassium hexaferrocyanide(II) ($K_4Fe(CN)_6$) (99.5 %), potassium hexacyanoferrate(III) ($K_3Fe(CN)_6$) (99.5 %) were obtained from Sigma-Aldrich (Germany). Olopatadine and eye drop (Patanol®) were acquired from NOVARTIS Turkey Inc. Deionized (DI) water was utilized in the experiments. The stock solution of 1.0 mM OLP was prepared via DI water.

Apparatus

Energy-dispersive X-ray analysis of the sample was conducted using a Quanta FEG 450 field emission scanning electron microscope. The sample's morphology was characterized by transmission electron microscopy (FEI TALOS F200S) operated at 200 kV. Raman spectrum of TiO_2 NPs was observed from Renishaw inVia with a 785 nm solid-state diode laser at 1.0 mW power and 10 s acquisition times. The diffused reflectance (DRS) analysis was conducted by a Shimadzu UV-2401 UV–Vis spectrophotometer.

Synthesis of TiO_2 nanoparticles

TiO_2 nanoparticles were synthesized by the microwave-assisted hydrothermal method (MWHT). As comparing the conventional hydrothermal method (HT), the MWHT also has several benefits as follows; i) shorter reaction time and ii) complete reaction at lower temperatures. Thus, the microwave reaction formation helps shorten the reaction time and form reactions at lower temperatures. The microwave process may also facilitate TiO_2 crystals to be developed, and microwave radiation can accelerate the TiO_2 nucleation. Moreover, low temperatures and power for microwave-assisted hydrothermal preparation may observe many morphological structures mentioned above. The Teflon-covered autoclave microwave-assisted hydrothermal vessel received 5.0 mL titanium isopropoxide, 5.0 mL 1.0 M NaOH, and 60.0 mL ultrapure water. A CEM Mars 5 microwave digestion machine was employed to prepare the reaction solution, forcefully agitated at room temperature for 30 minutes. Microwave-assisted hydrothermal synthesis was performed at 100 ^oC for 30 minutes with a microwave output of 380 W. White TiO_2 NPs were washed with ultrapure water and ethanol after centrifugation at 5000 rpm for 15 minutes. Subsequently, the powder was dried overnight at 70 ^oC [39].

Fabrication of NFN/TiO_2/SPE

Firstly, The as-synthesized TiO_2 nanoparticles (0.5 mg) and 1.0 % Nafion were homogeneously dispersed in 1.0 ml Milli-Q water by ultrasonication until a uniform TiO_2 dispersion was gained. Following this, a 10.0 µL of NFN/TiO_2 dispersion was coated onto the previously cleaned SPE surface by drop-casting method and dried at room temperature. NFN/TiO_2/SPE was mildly rinsed with Milli-Q water to remove the non-attached composite materials on the surface of SPE. Moreover, to compare the electrochemical performance of the prepared composite materials, the SPE surfaces were also modified with TiO_2 as precursor material.

Results and discussion

Characterization of TiO_2

FE-SEM, HR-TEM, and Raman spectroscopy techniques were implemented to characterize TiO_2 nanoparticles synthesized via the microwave hydrothermal method, and the obtained results were

exhibited in Fig. 1. In Fig. 1, the diffused reflectance spectrum of TiO_2 NPs was depicted. TiO_2 NPs' DRS spectra reflected a 380-800 nm light spectrum. At a wavelength of 383 nm, TiO_2 NPs exhibited a DRS signal. A transfer of electrons from the O 2p orbital to the Ti 3d orbital was presented by this high peak [40]. A Kubelka-Munk function was used to determine the bandgap values of this sample, and the Kubelka-Munk graph of produced TiO_2 NPs was illustrated in Fig 1. inset. TiO_2 NPs were of an estimated bandgap of 3.14 eV. Anatase TiO_2 has a theoretical bandgap of 3.2 eV [41].

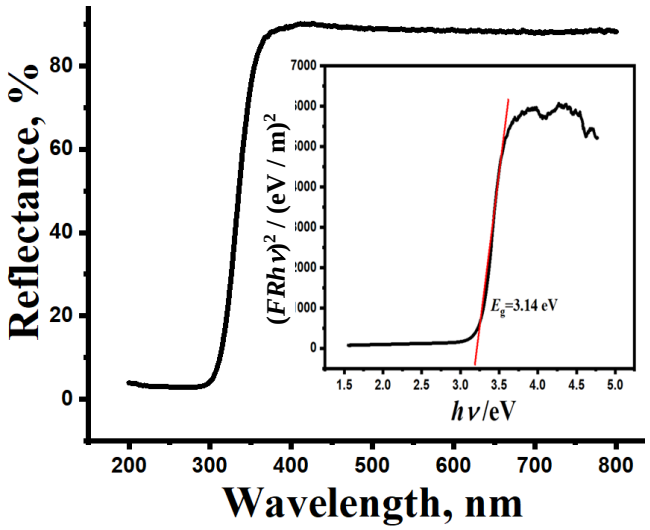

Figure 1. *DRS and hv / eV of synthesized TiO_2 NPs*

The TEM images of TiO_2 NPs were depicted in Fig. 2a and 2b. Aggregates with a nanoparticle diameter of 15 nm were detected in the TiO_2 sample. The d-spacing of the (101) and (110) planes of anatase structure corresponded to the lattice spacing of 0.318 and 0.325 nm, respectively.

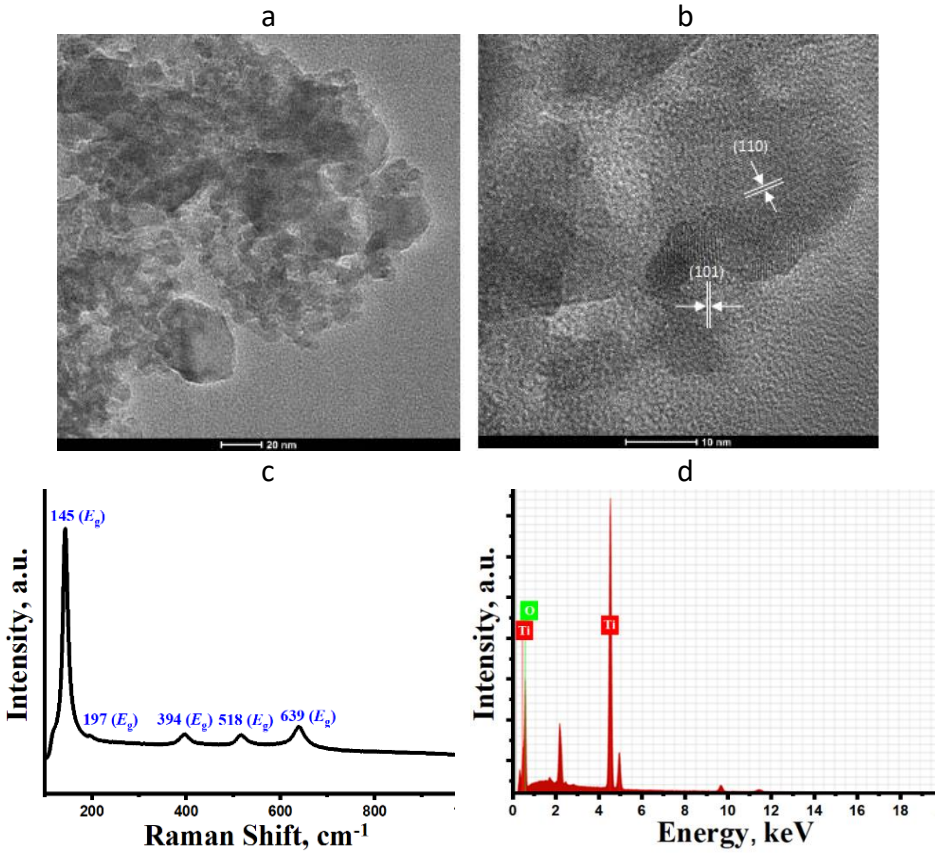

Fig. 2. TEM images (a, b), Raman spectra (c), and EDX spectra (d) of TiO_2

The Raman spectra of TiO_2 NPs are illustrated in Fig. 2c. The spectrum presented the five distinctive peaks of anatase TiO_2. The following peaks appeared: E_g = 145, 197, 394, 518, and 639 cm^{-1} [42]. The crystalline size of the material was likewise impacted by the Raman peak broadenings. The crystalline size of the material might be estimated using the Raman low frequency E_g mode peaks (143, 155 cm^{-1}). The TiO_2 NPs had a full-width hall maximum of 16 cm^{-1}. According to the Raman spectra, these predicted crystalline size estimates were likewise in excellent agreement with those computed according to Debye-Scherrer. The existence of elements was verified by energy-dispersive X-ray spectroscopy (Fig. 2d).

Electrochemical behavior of Olopatadine at NFN/TiO_2/SPE

The electrochemical performance of the modified sensing platforms was assessed by cyclic voltammetry (CV) in the presence of 0.1 M Britton-Robinson (B-R) buffer at pH 4.0 containing 100.0 µM OLP at a potential scan rate of 50.0 mV s^{-1}. As can be seen in Fig. 3, a well-defined oxidation signal of OLP at ~1.0V was achieved at bare SPE (blue line) and modified SPE surfaces with TiO_2 (yellow line) and NFN/TiO_2 (red line). The corresponding voltammetric curves represented by CV demonstrated that the modification of SPE surfaces by NFN/TiO_2 remarkably enhanced the sensitivity towards the OLP with an excellent electrocatalytic activity compared to that of bare SPE due to their larger surface areas. The corresponding oxidation current for OLP at NFN/TiO_2/SPE was 2.7 µA, which was 2.2 times greater than that of unmodified SPE. This significant enhancement in the voltammetric response of OLP with a negative oxidation potential shift that occurred at NFN/TiO_2/SPE could be assigned to the synergistic effect of NFN and metal oxides.

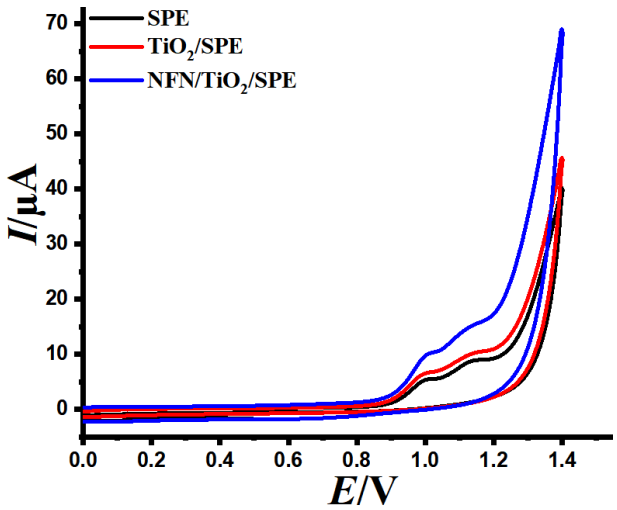

Fig. 3. *CVs of NFN/TiO_2/SPE (blue line), TiO_2/SPE (red line), and bare SPE (black line) electrode in pH 4.0 BR buffer ata scan rate of 50.0 mV s^{-1}.*

The ability of electron transfer rate of the NFN/TiO_2/SPE electrochemical sensors was evaluated by EIS using $[Fe(CN)_6]^{3-/4-}$ solution as a redox probe. They were obtained at different electrodes of the bare electrode, TiO_2/SPE, and NFN/TiO_2/SPE in the presence of 5.0 mM $[Fe(CN)_6]^{3-/4-}$ in 0.1 M KCl. By comparing different electrodes, the charge transfer resistance (R_{ct}) values were calculated to be 7.4, 5.8 and 2.2 kΩ for bare electrode, TiO_2/SPE, and NFN/TiO_2/SPE, respectively (Fig. 4). The results confirmed that the synergistic effect of TiO_2 and NFN in the modified electrode improved due to their properties, such as the increase in the conductivity of the electrode and the electron transfer. According to Fig. 4, the electrochemical reaction occurred more efficiently on NFN/TiO_2/SPE thanks to the least charge transfer resistance and the special electron transfer rate [32].

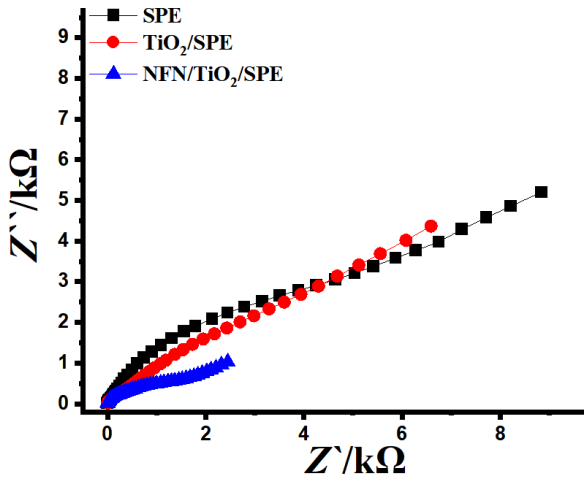

Fig. 4. *EIS responses at the bare electrode, TiO_2/SPE, and NFN/TiO_2/SPE in $[Fe(CN)_6]^{3-/4-}$ as redox probe containing 0.1 M KCl*

Optimization of experimental conditions

Investigation of pH and scan rate

The impact of pH upon the voltammetric response of OLP was investigated at NFN/TiO_2/SPE using a B-R buffer system in the varying pH range from 2.0 to 7.0. As depicted in Fig. 5a, the oxidation peak current of OLP increased gradually from 2.0 to 4.0 and then attained its maximum current value with a good peak shape at pH 4.0.

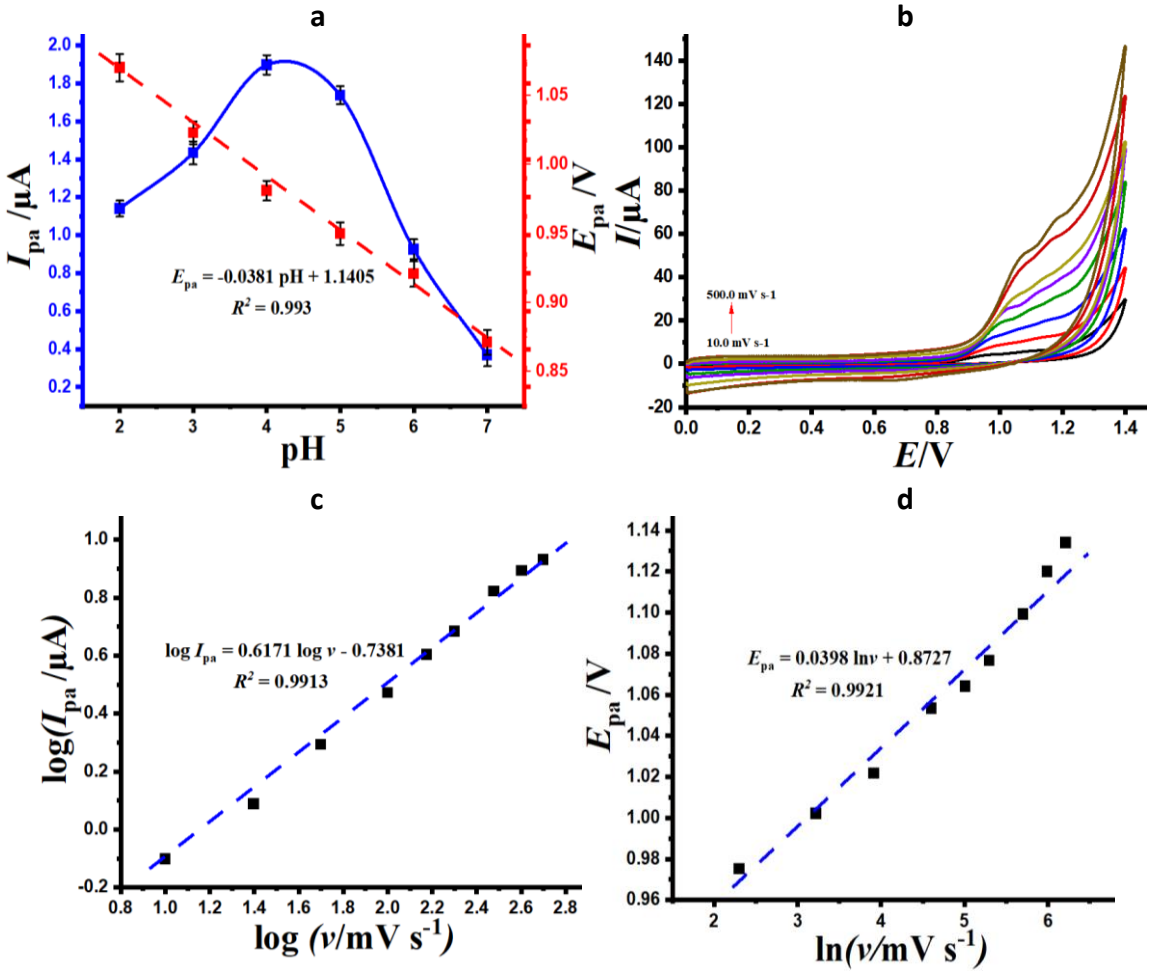

Fig. 5*. (a) Impact of varying pH values on the peak current of OLP; (b) CVs of 100.0 µM OLP on NFN/TiO_2/SPE in pH 4.0 B-R buffer at varying scan rates (10.0, 25.0, 50.0,100.0, 150.0, 200.0, 300.0, 400.0 and 500.0 mVs^{-1}); (c) The plot of the logIpa vs. log v obtained at the surface of NFN/TiO_2/SPE; (d) The plot of Epa vs. natural logarithm of scan rate for OLP*

Above pH >4.0, the corresponding peak current of OLP started to decrease continually until pH 7.0. Therefore, the best pH condition for OLP was selected as pH 4.0 for further analytical measurements. The linear curve equation that plotted the potentials against pHs was E_p =−0.0381pH+ 1.1405 (R^2 = 0.993). The slope attained for the principal oxidation peak in the first scan was 38.1 mV/pH, close to the theoretical value of 59 mV/pH. These results demonstrated that the transferred electron and proton numbers were equal[43].

The scan rate step is an essential parameter for determining the electrode reaction of the analyte at the working electrode. Fig. 5b exhibited the scan rate effect on the voltammetric response of OLP at NFN/TiO_2/SPE in 0.1 M B-R buffer (pH 4.0) at different scan rates ranging from 10.0 to 500.0 mV s^{-1}.The plot of the logarithm of the oxidation peak current (log I_{pa}) against the logarithm of the scan rate (log v) was found to be linear with the following regression equation: log I_{pa} = 0.6171 log v –0.7381 (R^2=0.9913), indicating a diffusion-controlled electrode reaction with a contribution of the adsorption (Fig. 5c).

Likewise, it exhibited that the oxidation peak potential (E_{pa}) of OLP shifted towards the positive direction with the scan rate's enhancement, which recommended the expected result for an irreversible electrode reaction. The number of electrons transferred in the oxidation step of OLP can be calculated by Laviron's equation from the slope of E_{pa} *vs.* ln v plot. The relationship between E_{pa} *vs.* ln v was expressed as: E_{pa}=0.0398 ln v + 0.8727 with a correlation coefficient of 0.9921. The number of electrons in the electro-oxidation of OLP was estimated to be ~1.25, demonstrating that the oxidetion reaction of OLP at NFN/TiO_2/SPE is of a single electron and proton transfer process. As a result, using pH scan and scan rate studies, a possible oxidation mechanism for OLP was illustrated in Scheme.2.

The amount of OLP absorbed on the surface of the NFN/TiO_2/SPE electrode was observed by the following equation:

$$I_p = \frac{nFQv}{4RT} = \frac{n^2F^2\tau v}{4RT} \quad (1)$$

Where n presents the number of electrons transferred, F is the Faraday's constant (96485 C mol^{-1}), A represents the area of the electrode, τ is the surface coverage of adsorbed substance, Q exhibits the quantity of charge consumed, and v is scan rate. Using the relationship of Ip with υ and integrating the peak area for OLP oxidation, the values of τwere calculated to be 20 µmol cm^{-2}.

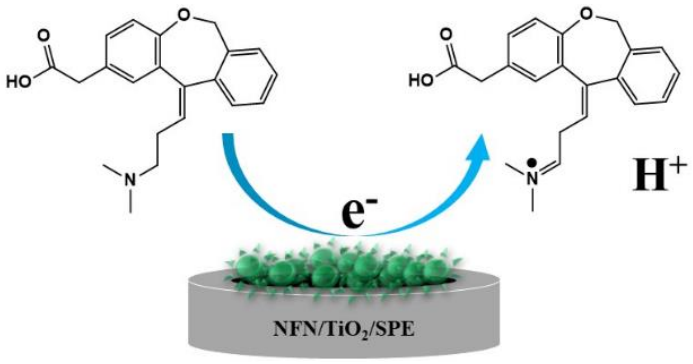

Scheme.2 *Possible electro-oxidation mechanism of OLP at NFN/TiO_2/SPE surface*

Effect of accumulation potential and time

Accumulation time and potential are essential aspects that significantly impact sensitivity in analyses. For an adsorption-controlled electrode reaction, optimizing pre-concentration steps of the target analyte on the electrode surface is an essential factor in enhancing the sensitivity of the proposed electroanalytical method. For this purpose, the effect of accumulation potential (E_{acc}) and

time (t_{acc}) on the oxidation responses of OLP was investigated by DPV at NFN/TiO_2/SPE. For E_{acc} optimization, the oxidation peak current of OLP was measured by applying various E_{acc} in the range of 0.2 to 0.9 V under a constant t_{acc} of 30 s (Fig. 6a). The maximum peak current for OLP was achieved at the E_{acc} of 0.50 V. In addition, the oxidation peak current of OLP at NFN/TiO_2/SPE enhanced piecemeal with increasing of t_{acc} from 15 to 60 s under fixed E_{acc} of 0.50 V and reached its maximum value at t_{acc} of 60 s (Fig. 6b). For longer t_{acc} values, the peak currents for OLP have almost remained stable due to the saturation of NFN/TiO_2/SPE with target molecules. Hence, E_{acc} value of 0.50 V and t_{acc} value of 60.0 s were determined as the optimal accumulation step parameters for further analytical measurements.

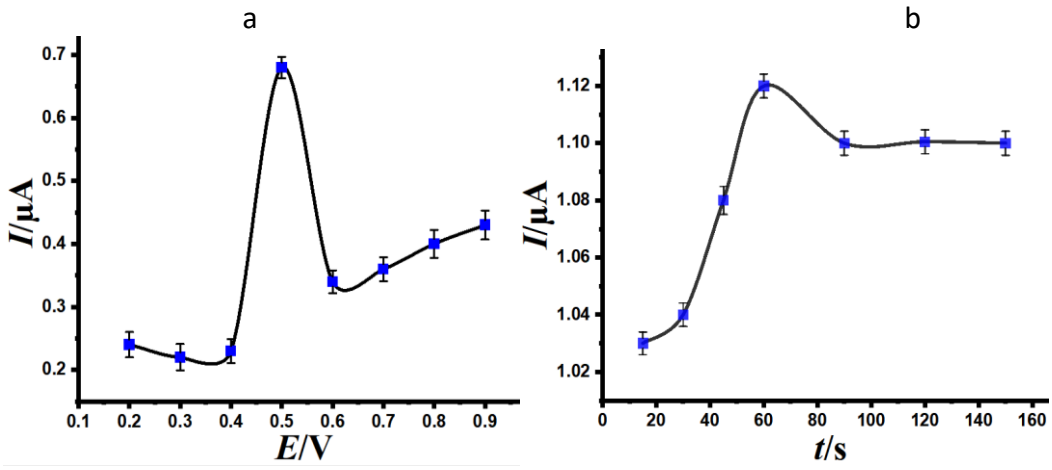

Fig. 6. *(a) Effect of t_{acc} upon the peak current with 0.5 V of E_{acc}, (b) Effect of E_{acc} upon the peak current with 60 s of t_{acc} for OLP in B-R (pH 4.0) on NFN/TiO_2/SPE*

Analytical performance

Differential pulse voltammetry (DPV) for OLP was implemented to enhance the sensitivity of the proposed electrochemical sensing platform. DPV investigated the analytical performance of developed NFN/TiO_2/SPE towards the different concentrations of OLP under optimized experimental conditions (such as pH of the supporting electrolyte, scan rate, accumulation potential, and time). Fig. 7 illustrated the DP voltammograms and the corresponding calibration curve by plotting the oxidation peak current against the increasing OLP concentration (COLP). Two linear calibration ranges from 0.01 to 0.07 and 0.07 to 14.66 µM for OLP were obtained at the surface of NFN/TiO_2/SPE with the following regression equations: I_{pa} = 3.101 C_{OLP} + 0.255 (R^2=0.9924) and I_{pa} = 0.211C_{OLP} + 0.5597 (R^2 = 0.9982). The sensitivity (slope) of the second linear segment for OLP decreased due to the kinetic limitations. The limit of detection (LOD) value for OLP was calculated as 7.0 nM (3.3Sb/m = 3) [24]. Here, Sb represents the standard deviation of the peak current (n = 10) of 0.01 µM olopatadine, and m is the slope of calibration plots. This improved sensing performance of NFN/TiO_2/SPE for OLP could be attributed to the synergic effect of NFN and metal oxide nanoparticles, which provided an enhanced conductivity, fast electron transfer, and large surface area. The analytical performance of the proposed sensing platform was compared with the similar developed electrochemical sensing platforms for the determination of OLP. The obtained analytical parameters were compared to similar reported analytical methods, which have been utilized to sense OLP (Table 1). The analytical performance of NFN/TiO_2/SPE, which was of wide linearity and low LOD value, exhibited to be much more appropriate than other comparative analytical methods towards the detection of OLP. The results suggested that NFN/TiO_2/SPE was of comparable analytical performance (linearity and LOD) towards the OLP (Table 2).

Table. 1. *A collation between diverse methods to detect OLP by the developed methods*

Method	Materials	Linear range, µM	LOD, µM	Ref.
Potentiometric	OLP–PM-CPE	3×10^{-5} - $\times10^{-2}$	1.39×10^{-5}	[44]
Potentiometric	Poly/ONOE	10^{-5} - 10^{-2}	5.0×10^{-6}	[45]
CV	HMDE	10^{-8} - 4.0×10^{-7}	5.7×10^{-9}	[46]
DPV	NFN/TiO_2/SPE	10^{-8} - 14.66×10^{-6}	7.01×10^{-8}	This work

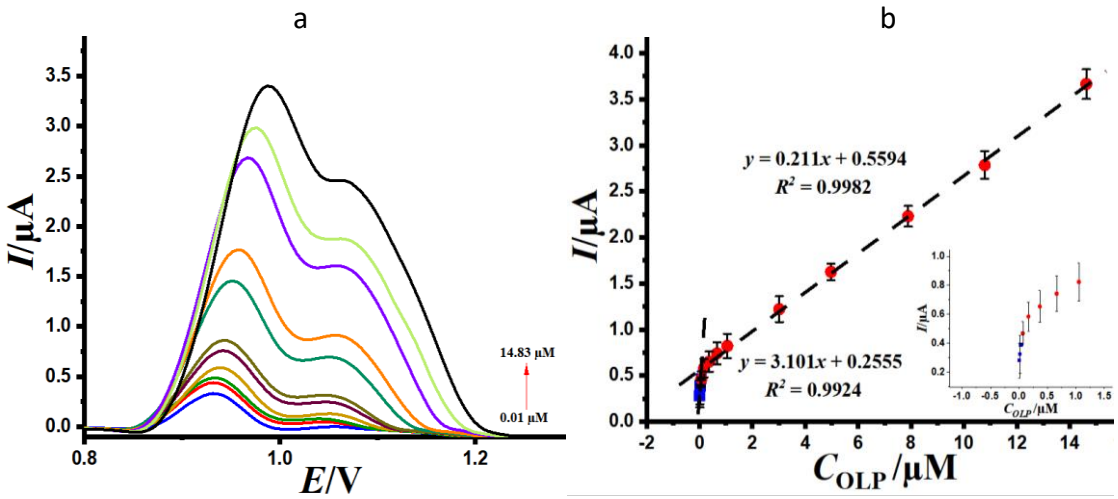

Fig. 7. *(a) DPVs of NFN/TiO_2/SPE in 0.1 M BR buffer at pH 4.0 containing different concentrations of OLP, (b) plots of I_p vs. OLP concentrations*

Table. 2. *The analytical parameters were obtained by electrochemical determination of OLP at NFN/TiO_2/SPE in 0.1 M B-R(pH 4.0)*

Parameters	NFN/TiO_2/SPE
Measured potential, mV	500
Measured time, s	60
Linear working range, µM	0.01-14.63
Slope, µA/µM	0.2188
R^2	0.9914
Intercept	0.4829
LOD, nM	10
LOQ, nM	33.4

Interference test study

The detection capability of the proposed sensing platform towards the OLP in the presence of various potential interfering agents, which have commonly been found in biological samples, was assessed by DPV under optimized experimental conditions. The results exhibited that a 100-fold excess of biological compounds (ascorbic acid, dopamine, glucose, and uric acid) and amino acids (l-cysteine and l-arginine) did not show no or negligible interference effect in the determination of OLP (Table 3).

Table 3. ***I****nfluence of various interfering agents on OLP (1.0 µM) at NFN/TiO_2/SPE (n = 4),* $C_{Interf\ agents}$ *:* C_{OLP} *= 100 : 1*

Interfering agents	RSD, %
Ascorbic acid	1.16
Dopamine	0.32
Glucose	0.52
Uric acid	0.91
l-cysteine	1.3
l-arginine	2.41

The corresponding relative errors for OLP were lower than ±2 %, which was correlated with the tolerance limit defined in the selectivity measurements, indicating that NFN/TiO_2/SPE has a promising selectivity for the determination of OLP.

Repeatability, reproducibility

To prove the repeatability of the developed electrochemical sensor, the five replicate DPV measurements for OLP were conducted using the same NFN/TiO_2/SPE in pH 4.0 B-R buffer containing 1.0 µM OLP under optimized accumulation conditions. Similarly, the NFN/TiO_2/SPE reproducibility was evaluated by monitoring the 1.0 OLP solution in pH 4.0 B-R using five independently prepared electrochemical sensors. The corresponding relative standard deviation (RSD) values for repeatability and reproducibility tests were found as 0.73 and 2.50 %, respectively, confirming that NFN/TiO_2/SPE has satisfactory repeatability and reproducibility towards the detection of OLP.

Real sample analysis

In real sample analysis, the eye drop sample with a spiked value of olopatadine was employed for the NFN/TiO_2/SPE capability. The obtained data by the standard addition method were tabulated in Table 4. Good recovery data 98.2 and 99.0 % confirmed the powerful ability of NFN/TiO_2/SPE in determining olopatadine in the real samples.

Table 4. *The results data relative to analysis of olopatadine in the real sample.*

Sample	*C* / µM		RSD, %	Recovery, %
	Added	Found		
Eye drop	2.0	1.98	3.49	99.0
	4.0	3.93	4.21	98.2

Conclusions

In this paper, a new method for fabricating a selective and straightforward electrochemical sensor based on NFN/TiO_2 was proposed for future electrochemical sensing applications to determine the trace level of OLP in the eye drop sample. The modification of NFN/TiO_2 on SPE dramatically enhanced the electrocatalytic activity towards OLP oxidation due to its large surface area, improved electron transfer kinetics, and high adsorption ability. NFN/TiO_2/SPE illustrated a highly desirable analytical performance at the concentration ranges of 0.01 to 0.07 and 0.07 to 14.63 µM with a meager detection limit of 7.0 nM. The developed portable sensing platform also presents several advantages, such as high reproducibility, repeatability, and appropriate selectivity with an RSD of less than 5 %. The feasibility of the proposed sensing platform was successfully tested in an eye drop sample with adequate accuracy, precision results, and recovery of 98.2-99.0 %. It can be speculated that the proposed novel NFN/TiO_2/SPE-based electrochemical sensing platform could be utilized as an alternative analytical approach with a high potential to determine antiviral agents such as OLP in future clinical applications.

Acknowledgments: *This work was supported by the Scientific Research Projects Commission of Ankara University (Project Number: 21B0237005 and 19L0237004).*

References

[1] K. Ohmori, K. Hasegawa, T. Tamura, K. Miyake, M. Matsubara, S. Masaki, A. Karasawa, N. Urayama, K. Horikoshi, J. Kajita, *Arzneimittelforschung* **54** (2004) 12, 809-829. https://doi.org/10.1055/s-0031-1297036

[2] S. Dey, Y. Reddy, B. Swetha, S. Kumar, P. Murthy, S. Sahoo, D. Kumar, S. Patro, S. Mohapatra, *International Journal of Pharmacy and Pharmaceutical Sciences* **2(4)** (2010) 212-218. http://www.ijppsjournal.com/Vol2Suppl4/812.pdf

[3] D. Jain, P. Basniwal, *Journal of Pharmaceutical Research* **12(2)** (2013) 48-52. https://www.researchgate.net/publication/253240922_Spectrophotometric_Determination_of_Olopatadine_Hydrochloride_in_Eye_Drops_and_Tablets

[4] M. M. Annapurna, G. H. Bindu, I. Divya, *Drug Invention Today* **4** (2012) 8.

[5] S. K. Raul, B. Kumar, A. K. Patnaik, N. N. Rao, *Asian Journal of Research in Chemistry* **5(11)** (2012) 1395-1398. https://ajrconline.org/AbstractView.aspx?PID=2012-5-11-16

[6] P. K. Basniwal, D. Jain, *Journal of Analytical Science and Technology* **4(1)** (2013) 12. https://doi.org/10.1186/2093-3371-4-12

[7] S. Tajik, Y. Orooji, Z. Ghazanfari, F. Karimi, H. Beitollahi, R.S. Varma, H.W. Jang, M. Shokouhimehr, *Journal of Food Measurement and Characterization* **15** (2021) 3837-3852. https://doi.org/10.1007/s11694-021-00955-1

[8] E. Mirmomtaz, A. Asghar Ensafi, H. Karimi-Maleh, *Electroanalysis* **20(18)** (2008) 1973-1979. https://doi.org/10.1002/elan.200804273

[9] A. A. Ensafi, H. Karimi-Maleh, *Drug testing and analysis* **3(5)** (2011) 325-330. https://doi.org/10.1002/dta.232

[10] [A. A. Ensafi, H. Karimi-Maleh, S. Mallakpour, *Electroanalysis* **23(6)** (2011) 1478-1487. https://doi.org/10.1002/elan.201000741

[11] H. Karimi-Maleh, M. Keyvanfard, K. Alizad, M. Fouladgar, H. Beitollahi, A. Mokhtari, F. Gholami-Orimi, *International Journal of Electrochemcal Science* **6(12)** (2011) 6141-6150. http://www.electrochemsci.org/papers/vol6/6126141.pdf

[12] J. Raoof, R. Ojani, H. Karimi-Maleh, *Journal of Applied Electrochemistry* **39(8)** (2009) 1169-1175. https://doi.org/10.1007/s10800-009-9781-x

[13] M. A. Khalilzadeh, H. Karimi-Maleh, A. Amiri, F. Gholami, *Chinese Chemical Letters* **21(12)** (2010) 1467-1470. https://doi.org/10.1016/j.cclet.2010.06.020

[14] S. Tajik, Y. Orooji, F. Karimi, Z. Ghazanfari, H. Beitollahi, M. Shokouhimehr, R. S. Varma, H. W. Jang, *Journal of Food Measurement and Characterization* **15** (2021) 4617-4622. https://doi.org/10.1007/s11694-021-01027-0

[15] Y. Orooji, P. N. Asrami, H. Beitollahi, S. Tajik, M. Alizadeh, S. Salmanpour, M. Baghayeri, J. Rouhi, A. L. Sanati, F. Karimi, *Journal of Food Measurement and Characterization* **15** (2021) 4098-4104. https://doi.org/10.1007/s11694-021-00982-y

[16] M. Alizadeh, P.A. Azar, S.A. Mozaffari, H. Karimi-Maleh, A.-M. Tamaddon, *Frontiers in Chemistry* **8** (2020) 814. https://doi.org/10.3389/fchem.2020.00814

[17] M. Al Sharabati, R. Abokwiek, A. Al-Othman, M. Tawalbeh, C. Karaman, Y. Orooji, F. Karimi, *Environmental Research* **202** (2021) 111694. https://doi.org/10.1016/j.envres.2021.111694

[18] F. Karimi, A. Ayati, B. Tanhaei, A. L. Sanati, S. Afshar, A. Kardan, Z. Dabirifar, C. Karaman, *Environmental Research* **203** (2021) 111753. https://doi.org/10.1016/j.envres.2021.111753

[19] A. Aykan, O. Karaman, C. Karaman, N. Atar, M. L. Yola, *Surfaces and Interfaces* **25** (2021) 101293. https://doi.org/10.1016/j.surfin.2021.101293

[20] C. Karaman, E. Bayram, O. Karaman, Z. Aktaş, *Journal of Electroanalytical Chemistry* **868** (2020) 114197. https://doi.org/10.1016/j.jelechem.2020.114197

[21] O. Karaman, H. Özdogan, Y.A. Üncü, C. Karaman, A.G. Tanır, *Kerntechnik* **85(5)** (2020) 401-407. https://doi.org/10.3139/124.200022

[22] H. Karimi-Maleh, A. Ayati, R. Davoodi, B. Tanhaei, F. Karimi, S. Malekmohammadi, Y. Orooji, L. Fu, M. Sillanpää, *Journal of Cleaner Production* **291** (2021) 125880. https://doi.org/10.1016/j.jclepro.2021.125880
[23] E. Vatandost, A. Ghorbani-HasanSaraei, F. Chekin, S. N. Raeisi, S.-A. Shahidi, *Food Chemistry: X* **6** (2020) 100085. https://doi.org/10.1016/j.fochx.2020.100085
[24] M. Mehmandoust, N. Erk, C. Karaman, F. Karimi, S. Salmanpour, *Micromachines* **12(11)** (2021) 1334. https://doi.org/10.3390/mi12111334
[25] H. Karimi-Maleh, F. Karimi, L. Fu, A. L. Sanati, M. Alizadeh, C. Karaman, Y. Orooji, *Journal of Hazardous Materials* **423** (2021) 127058. https://doi.org/10.1016/j.jhazmat.2021.127058
[26] C. Karaman, *Topics in Catalysis* (2021). https://doi.org/10.1007/s11244-021-01500-6
[27] C. Karaman, O. Karaman, N. Atar, M. L. Yola, S*Physical Chemistry Chemical Physics* **23(22)** (2021) 12807-12821. https://doi.org/10.1039/D1CP01726H
[28] C. Karaman, Z. Aktaş, E. Bayram, O. Karaman, Ç. Kızıl, *ECS Journal of Solid State Science and Technology* **9(7)** (2020) 071003. https://doi.org/10.1149/2162-8777/abb192
[29] C. Karaman, O. Karaman, B. B. Yola, İ. Ulker, N. Atar, M. L. Yola, *New Journal of Chemistry* 45 (2021) 11222-11233. https://doi.org/10.1039/D1NJ02293H
[30] H. Medetalibeyoğlu, M. Beytur, S. Manap, C. Karaman, F. Kardaş, O. Akyıldırım, G. Kotan, H. Yüksek, N. Atar, M.L. Yola, *ECS Journal of Solid State Science and Technology* **9(10)** (2020) 101006. https://doi.org/10.1149/2162-8777/abbe6a
[31] N. H. Khand, A. R. Solangi, S. Ameen, A. Fatima, J .A. Buledi, A. Mallah, S. Q. Memon, F. Sen, F. Karimi, Y. Orooji, *Journal of Food Measurement and Characterization* **15** (2021) 3720-3730. https://doi.org/10.1007/s11694-021-00956-0
[32] M. Alizadeh, M. Mehmandoust, O. Nodrat, S. Salmanpour, N. Erk, *Journal of Food Measurement and Characterization* **15** (2021) 5622-5629. https://doi.org/10.1007/s11694-021-01128-w
[33] H. Karimi-Maleh, Y. Orooji, F. Karimi, M. Alizadeh, M. Baghayeri, J. Rouhi, S. Tajik, H. Beitollahi, S. Agarwal, V. K. Gupta, *Biosensors and Bioelectronics* **184** (2021) 113252. https://doi.org/10.1016/j.bios.2021.113252
[34] L. Hu, C.-C. Fong, X. Zhang, L. L. Chan, P.K. Lam, P. K. Chu, K.-Y. Wong, M. Yang, *Environmental Science and Technology* **50(8)** (2016) 4430-4438. https://doi.org/10.1021/acs.est.5b05857
[35] M. Khodari, E. Rabie, H. Assaf, *International Journal of Science and Research* **5(11)** (2015) 1501-1505. https://www.ijsr.net/get_abstract.php?paper_id=ART20163056
[36] A. Mao, H. Li, Z. Cai, X. Hu, *Journal of Electroanalytical Chemistry* **751** (2015) 23-29. https://doi.org/10.1016/j.jelechem.2015.04.034
[37] A. A. Ensafi, E. Khoddami, B. Rezaei, H. Karimi-Maleh, *Colloids and Surfaces B: Biointerfaces* **81(1)** (2010) 42-49. https://doi.org/10.1016/j.colsurfb.2010.06.020
[38] S. Cheraghi, M. A. Taher, H. Karimi-Maleh, F. Karimi, M. Shabani-Nooshabadi, M. Alizadeh, A. Al-Othman, N. Erk, P. K. Y. Raman, C. Karaman, *Chemosphere* **287(2)** (2021), 132187. https://doi.org/10.1016/j.chemosphere.2021.132187
[39] M. Mehmandoust, S. Çakar, M. Özacar, S. Salmanpour, N. Erk, *Topics in Catalysis* (2021). https://doi.org/10.1007/s11244-021-01479-0
[40] J.-H. Huang, P. Y. Hung, S.-F. Hu, R.-S. Liu, *Journal of Materials Chemistry* **20(31)** (2010) 6505-6511. http://doi.org/10.1039/C0JM00549E
[41] B. Roose, S. Pathak, U. Steiner, *Chemical Society Reviews* **44(22)** (2015) 8326-8349. https://doi.org/10.1039/C5CS00352K
[42] T. K. Das, P. Ilaiyaraja, P. S. Mocherla, G. Bhalerao, C. Sudakar, *Solar Energy Materials and Solar Cells* **144** (2016) 194-209. https://doi.org/10.1016/j.solmat.2015.08.036

[43] T. Zabihpour, S.-A. Shahidi, H. Karimi-Maleh, A. Ghorbani-Hasan Saraei, *Journal of Food Measurement and Characterization* **14** (2020) 1039-1045. https://doi.org/10.1007/s11694-019-00353-8

[44] M. M. Abdel-Moety, *Der Pharmacia Lettre* **7(9)** (2015) 285-294. https://www.researchgate.net/publication/339102987_Carbon_paste_ion-selective_electrodes_for_the_determination_of_olopatadine_hydrochloride_in_bulk_and_pharmaceutical_dosage_forms/link/5e3d6d88299bf1cdb9163a01/download

[45] M. M. Sebaiy, M. A. Elmosallamy, M. M. Elhenawee, M. K. Alshuwaili, , *Microchemical Journal* **147** (2019) 170-175. https://doi.org/10.1016/j.microc.2019.03.030

[46] N. Sreedhar, A. Sreenivasulu, M. S. Kumar, M. Nagaraju, *Journal of Pharmaceutical Sciences and Research* **3(8)** (2012) 2517-2521. http://dx.doi.org/10.13040/IJPSR.0975-8232.3(8).2517-21